PHYS180 Project 2
Understanding Diffusion

Owen Morehead, Karoli Clever, Rey Cervantes

April 12, 2021

1 Diffusion in 1D

Steady state solution of the diffusion equation in 1 dimension

Particle starts at point $x = L$ and performs random walk. If particle hits origin its absorbed ($x = 0 \rightarrow C(x) = 0$). If it steps to the right its restarted at $x = L$ ($C(x > L) = 0$). Calculate the density of particles as a function of x in steady state, $C(x)$. Normalize it so that density is unity, $C(x) = 1$ at $x = L$.

Let us start with the diffusion equation:

$$\frac{\partial C}{\partial t} = D\nabla^2 C \tag{1}$$

and in 1D,

$$\frac{\partial C}{\partial t} = D\frac{\partial^2 C}{\partial x^2}. \tag{2}$$

Steady state means there is no change in concentration over time:

$$\frac{\partial C}{\partial t} = 0 \tag{3}$$

and therefore,

$$D\frac{\partial^2 C}{\partial x^2} = 0. \tag{4}$$

We can solve this second order, homogeneous differential equation fairly easily, noting that the second derivative of a line is 0.

$$C(x) = ax + b \tag{5}$$

Utilizing our boundary conditions:

$$C(x = 0) = 0 = b. \rightarrow \boxed{\text{b = 0}} \tag{6}$$

$$C(x = L) = 1 = a(L). \rightarrow \boxed{\text{a = 1/L}} \tag{7}$$

We have our linear solution to the differential equation that is the steady state concentration of particles as a function of x:

$$\boxed{\text{C(x) = x/L}} \tag{8}$$

Comparing this to the numerical result in SteadyStatehints.py, we see confirmation in that there is a linear relationship between the concentration of particles and their position in x. There are 0 particles at $x = 0$ and unity at $x = L$. This is what we see from both our analytical and numerical solution. This means the particles move from $x = L$ to $x = 0$ and as they get closer to $x = 0$ their concentration decreases linearly in x until $C(x) = 0$ at $x = 0$. An image of the numerical solution is shown in Figure 1.

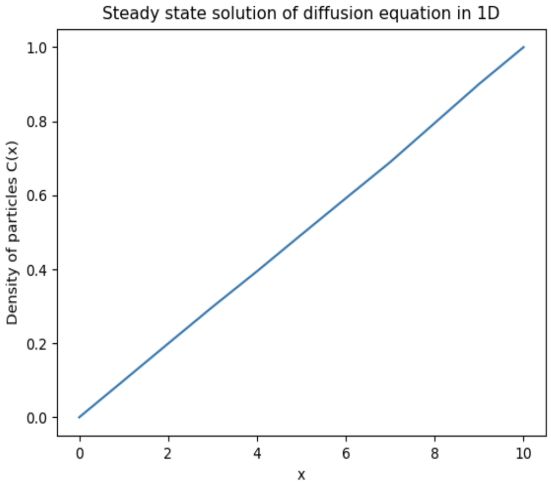

Figure 1: Steady state solution to the diffusion equation in 1D. Density of particles decreases linearly from C(x) = 1 at x = L = 10, to C(x) = 0 at x = 0.

As we saw, the density of particles varies with position giving rise to a gradient in density. An example of a biological technique that makes use of gradients in the density of small molecules is *density gradient centrifugation*. This is a technique used to separate cells or substances based on their shape and size. A centrifuge machine is used which spins liquid solutions at a high speed. The mixture experiences a centrifugal force, causing more dense particles to move to the outside edge of the sample as they are heavier and can carry farther by their inertia. Less dense particles settle towards the center of the sample, ultimately creating a solution that is sorted by particle density (https://www.akadeum.com/blog/density-gradient-centrifugation/). If the spinning speed is constant and therefore creates a constant centrifugal force, such density gradients will be maintained in steady state as in the above problem. Over the timescale used in this technique, the density or mass of particles does not change. Therefore if a constant centrifugal force is applied, the density gradient will be maintained in a steady state as long as no other chemical reactions are taking place. Should the constant centrifugal force stop, on the other hand, the steady state will not be maintained, and the separated components will slowly mix again in the solution.

The History of Density Gradient Centrifugation

Cesium chloride (CsCl) density gradient centrifugation (DGC) was first developed by M. Meselson, F. Stahl, and J. Vinograd in the early 1950s at Caltech. The method enables scientists to separate substances based on size, shape, and density, and in this case, a particular type of DGC, isopycnic centrifugation was developed. It used a solution of cesium chloride to separate DNA molecules based on density alone. Previous to this method, scientists had no other way to separate macromolecules that were of similar size but with different densities. This method was primarily developed to determine how DNA replicates and allowed scientists to isolate DNA and other macromolecules by density alone (Hernandez, V. 2017). DGC still requires the use of a centrifuge. This instrument spins mixtures in a rotor to concentrate or separate materials. Centrifugal force causes components of a mixture to separate by size, since larger components will experience a bigger centrifugal force than any smaller components. DGC is performed via an analytical ultracentrifuge, developed by T. Svedberg, Uppsala University, Sweden. Ultracentrifuges can spin samples approximately 5 times faster, with more force being exerted on the sample. This provides clearer separation and causes solutions to form density gradients. These form in solution when the density of that solution gradually increases and moves farther from the centrifuge rotor. When performing DGC, researchers use the ability to observe their samples during centrifugation and are able to directly watch the order that the components of their samples separate over a specific time (Cooney et al. 1985).

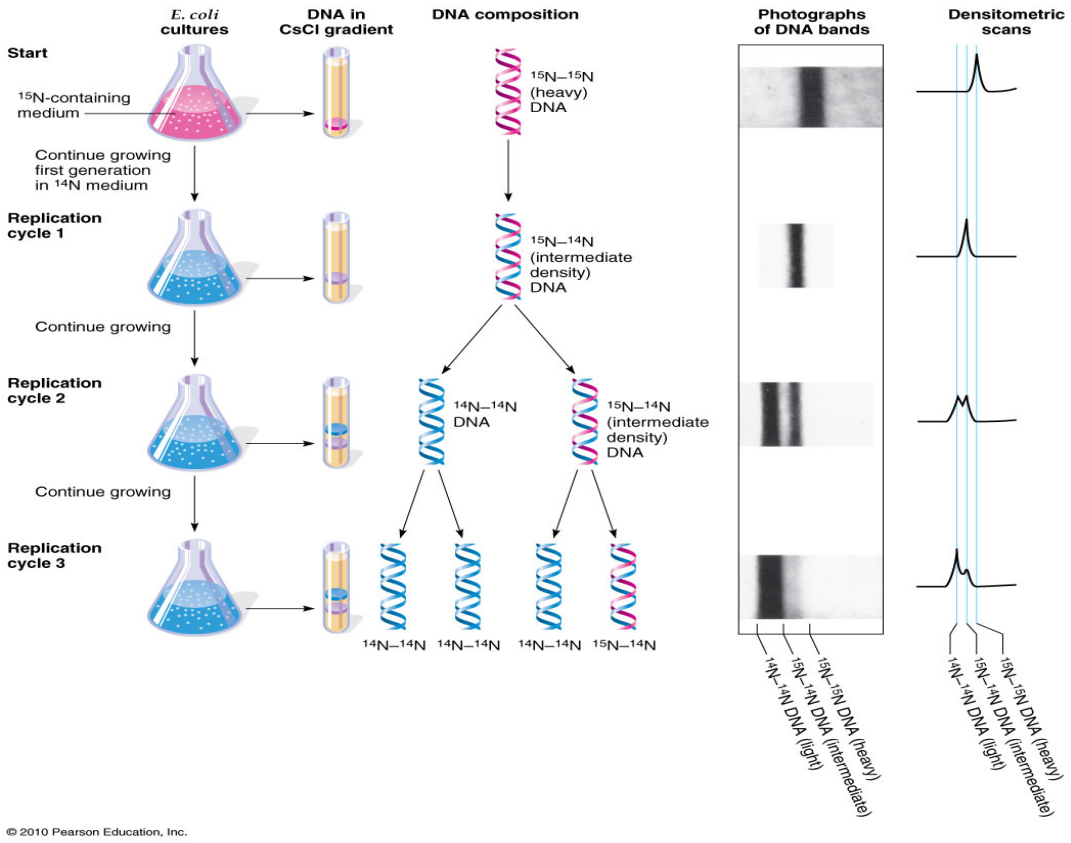

Figure 2: Method of *E. coli* DNA replication of cultures centrifuged with a density gradient CsCl, showing the DNA bands visible in the test tubes and in the photoanalysis and scans (Pearson Education Inc., 2010).

Meselson and Stahl came up with the hypothesis, that they could tag DNA with heavy elements as it replicated, then tracing the tag over many replication cycles to see which role the original DNA molecules played in replication. The heavy elements would not significantly alter the DNA´s chemical properties, but increase the weight of the DNA, yet not the size of the molecule. This meant, that they would only increase the density of the original DNA. Once DNA replicated, the samples would contain some of the original heavy DNA and some light DNA. Meselson and Stahl chose a cesium salt solution because it needed to be dense enough for the DNA molecules to float before the centrifugation process, yet mild so that samples would survive, and it spontaneously forms a density gradient after ultracentrifugation. The CsCl solution was centrifuged for many hours, and the resulting force gradually pushed the CsCl particles toward the bottom of the tube with the density of the CsCl increasing along a gradient down the tube. This CsCl density range was greater than the difference in densities between the heavy and light DNA being separated. The scientists centrifuged the samples until the DNA suspended in separate parts of the solution and stopped at an equilibrium point (Hernandez, V. 2017).

This method was called equilibrium sedimentation, by which particles in a solution reach a point where they reach their isopycnic position. This means that the centrifugal force pushing the particles down equals the force of the solution pushing up, and hence the particles will stop moving in the solution. The density of different DNA molecules is determined based on where they reach equilibrium and stop moving when their density matched the density of the surrounding solution (Hernandez, V. 2017). The particle bands that formed during DGC have Gaussian or normal distributions that are symmetric about the mean average value. For the DNA band, the number of DNA molecules greater than the mean density equals the number of DNA molecules less than the mean density, and the width of the band is inversely proportional to the centrifugal force. The width of the band relates inversely to the rate the density increases along the density gradient. The steeper the density gradient is, the sharper the band, which allow for more accurate measure-

ments because the densities of the DNA molecules in the band are closer to the mean density. The width of the band relates to the molecular weight and mean density of the molecules in that band (Farrell et al., 2010). Scientists also use density gradient centrifugation in a cesium solution to purify plasmids, circular pieces of bacterial DNA used for genetic engineering. Scientists still use density gradient centrifugation with cesium chloride to analyze DNA and RNA.

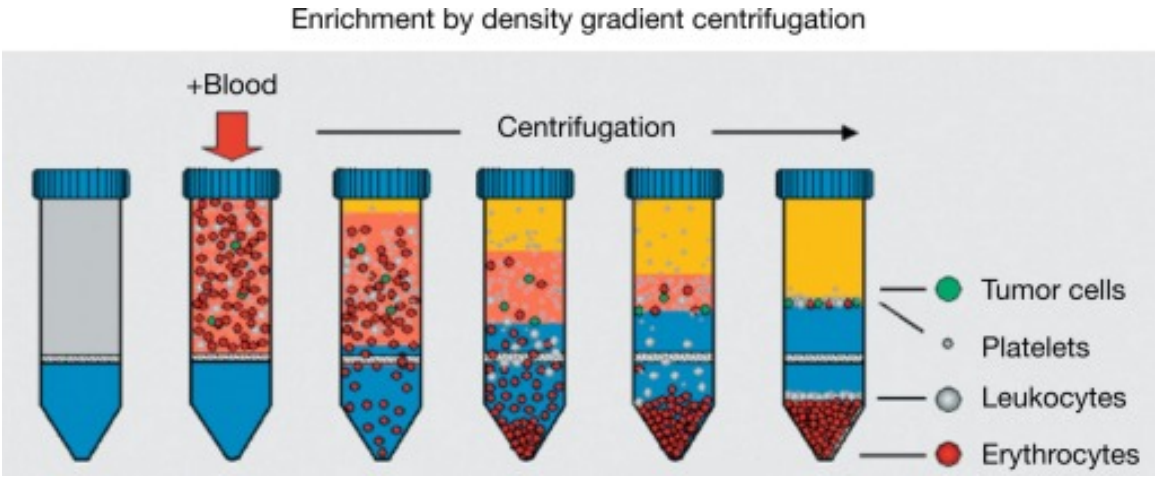

(a)

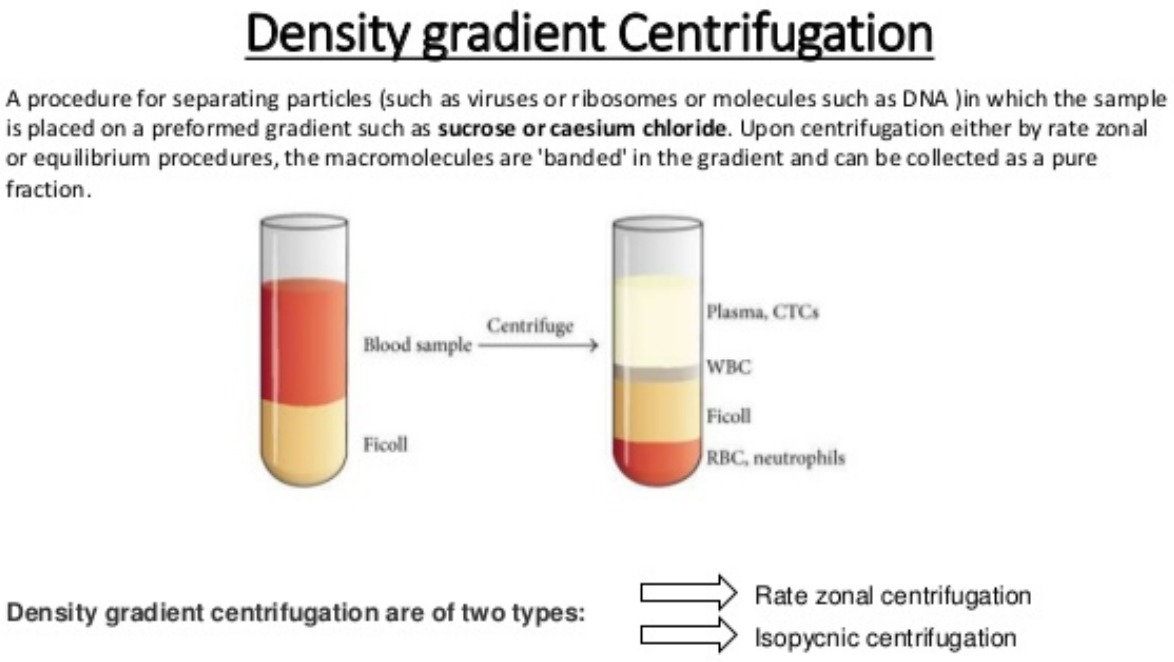

(b)

Figure 3: (a) Different stages of density gradient centrifugation used in the separation of tumor cells, leukocytes and erythrocytes (Lianidou et al., 2018). (b) Separation of blood plasma, white and red blood cells via DGC (SlideShare.net, 2018).

2 Diffusion in 3D

Probability of capture by a spherical adsorber by diffusion

Comments were added to the code in sphere.py which explain how the probability of capture by a spherical adsorber by diffusion works.
Utilizing equations 1 and 3, the we can find the steady state solution to the diffusion equation in 3D for this problem that involves spherical symmetry. The steady state diffusion equation is written as:

$$\frac{1}{r^2}\frac{d}{dr}(r^2\frac{dC}{dr}) = 0. \tag{9}$$

Which has the solution:

$$C(r) = \begin{cases} \frac{C_m}{1-a/b}(1-\frac{a}{r}) & a \leq r \leq b \\ \frac{C_m}{c/b-1}(\frac{c}{r}-1) & b \leq r \leq c \end{cases} \tag{10}$$

On a similar note, the radial flux is given by:

$$J_r(r) = \begin{cases} \frac{-DC_m}{1-a/b}(\frac{a}{r^2}) & a \leq r \leq b \\ \frac{DC_m}{c/b-1}(\frac{c}{r^2}) & b \leq r \leq c \end{cases} \tag{11}$$

To find the probability that a particle released at $r = b$ will be adsorbed at $r = a$, the ratio must be taken of the diffusion current from the spherical shell source to the inner adsorber to the sum of the diffusion currents from the spherical shell source to the inner adsorber and to the outer adsorber.

This ratio is given by:

$$\frac{I_{in}}{I_{in} + I_{out}} = \frac{a(c-b)}{b(c-a)} \tag{12}$$

In the sphere.py file, we set the outer radius to the value of 40 (our c), the starting radius to the value of 20 (our b), and the absorb radius to the value of 10 (our a). The numerical output that results in the code is 0.315. This is the probability of our particle being adsorbed at a from b in the simulation. When using the same parameters for a, b, and c to Equation 12, we have the analytical solution of 0.33.

Varying the parameter of c in the code, we can further verify the analytical solution. Keeping a at 10 and b at 20, but changing c to 30 yields 0.2443. Those same parameters in Equation 12 yields 0.25. Changing c to 50 in the code yields 0.3528. Equation 12 gives us 0.38. Changing c to 100 in the code yields 0.416 and Equation 12 gives 0.44. As a final test, we changed c to be 1000 in the code. Unfortunately, running this to completion would take far too long, but we did receive one output of 0.48, which was close to 0.49– the result from Equation 12. Theoretically, as c goes to infinity, the probability becomes a/b, which would be 0.5 if $a = 10$ and $b = 20$. With these trials varying c in our code, we have verified the analytical solution.

Biological examples of this kind of process:
The cell's plasma membrane and nuclear membranes are great examples of absorbing sphere models. Absorption of a random walker would be certain molecules that are needing to pass these membranes for important cell functions and replication. The membranes have specific pores and channels for the transport and reception of such molecules or in this case "walkers". The plasma membrane is selectively permeable, and hydrophobic molecules as well as small polar molecules can diffuse through the lipid layer at any location. Ions and large polar molecules can't pass the membrane and need specific transport channels that facilitate entry and exit through the membrane by selective coupling and conformation changes. Some are integral membrane proteins which will enable ions and large polar molecules to pass through the membrane by this passive or active type of transport forming gated channels that guide the transport rate in and out of the cell or nucleus. We can also find proteins which form these types of gated channels may be utilized to enable the transport of water and other hydrophilic molecules (Murphy et al., 2016).

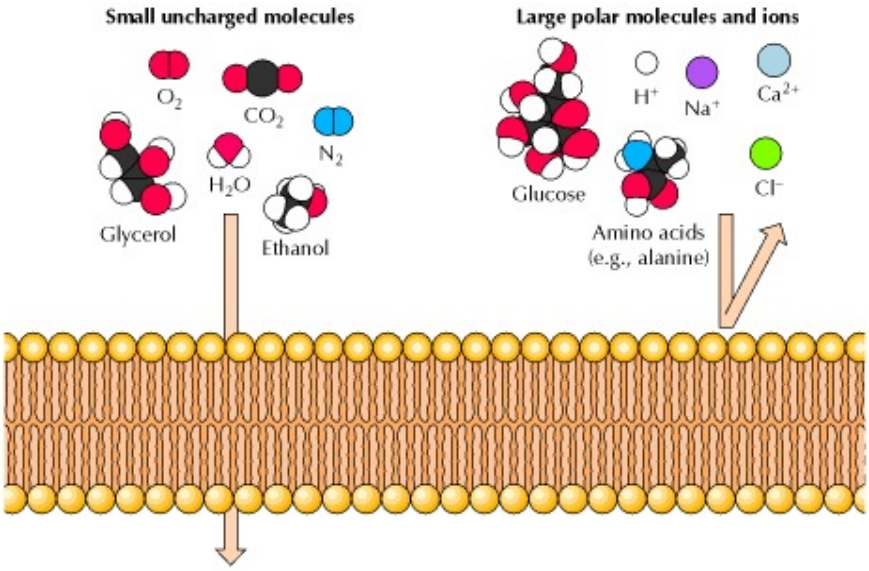

Figure 4: Molecules such as O_2, CO_2, N_2, and H_2O can diffuse through the plasma and nuclear membrane. Large molecules that are polar as well as many ions need other transport mechanisms in the cell membrane to enter or leave the cell. (ncbi.nlm.nih.gov, 2021)

Another form of transport is facilitated or passive transport, where hydrophilic molecules bind to a carrier protein, yet in active transport, hydrophilic molecules also bind to a carrier protein, but energy, usually in form of ATP produced through glycolysis or oxidative phosphorylation, is used to transport the molecules against their concentration gradient. Indirect energy sources are used in some cases, such as oxidation-reduction reactions where the change of electron states release the energy that is used. Specific ions are common in secondary transport systems, generating an electrochemical gradient. Bulk transport mechanisms enable large molecules or larger objects to cross the plasma membrane. The process of exocytosis exports large molecules from the cell and receptor mediated endocytosis allows specific large molecules to enter. Other forms of endocytosis allow liquids to be taken in by a process called pinocytosis and large objects, such as debris or microorganisms, to be taken in by phagocytosis (Projects.ncsu.edu, 2021).
Only small uncharged molecules can diffuse freely through phospholipid bilayers. Small nonpolar molecules, for example O_2 and CO_2, are soluble in this bilayer and cross cell membranes. Small uncharged polar molecules, such as H_2O, also can diffuse through membranes, yet larger uncharged polar molecules, such as glucose, cannot cross through it. Charged molecules, such as ions, are unable to diffuse through a phospholipid bilayer regardless of size, and this includes H^+ ions. For example the sodium-potassium pump which is crucial for cell functions and is found in many plasma membranes. Also powered by ATP, it moves sodium and potassium ions in opposite directions, each against its concentration gradient. In a single cycle of the pump, three sodium ions are extruded from and two potassium ions are imported into the cell. These ions have to couple in the opening of the pump in exact configurations and conformations for the pump to import and export the according ions (Opentextbc.ca, 2021).

The nuclear membrane has nuclear pores, where each pore is a large complex of proteins that allows small molecules and ions to freely pass, or diffuse, into or out of the nucleus. Furthermore, these pores allow necessary proteins to enter the nucleus from the cytoplasm, but the proteins have special sequences that indicate they belong in the nucleus, called tags, known as nuclear localization signals. RNA transcribed in the nucleus, as well as proteins that are destined to enter the cytoplasm of the cell have nuclear export sequences that tag them for release through the nuclear pores (Nature.com, 2021). This means any boundary conditions would have to facilitate the passing and diffusion of small nonpolar molecules, such as O_2 and CO_2, and small uncharged polar molecules, such as H_2O, as well as these tagged proteins. The average human nuclear pore channel is approximately 5.2 nanometers.

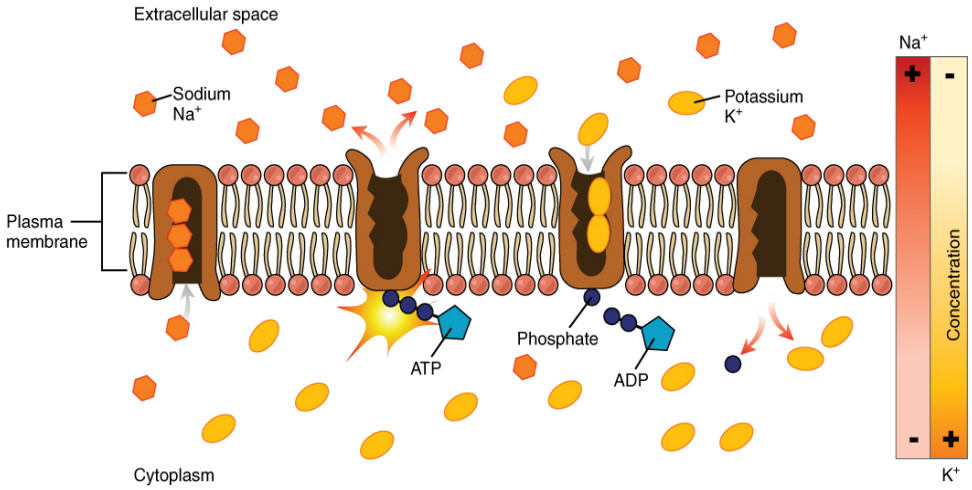

Figure 5: Sodium-Potassium pump in the cell's plasma membrane showing the different concentrations of both sodium and potassium inside and outside the cell. In combination with the use of energy via ATP, the pump selectively fits three sodium molecules and two potassium molecules in its channel before it can transport in or out of the cytoplasm (opentextbc.ca, 2021).

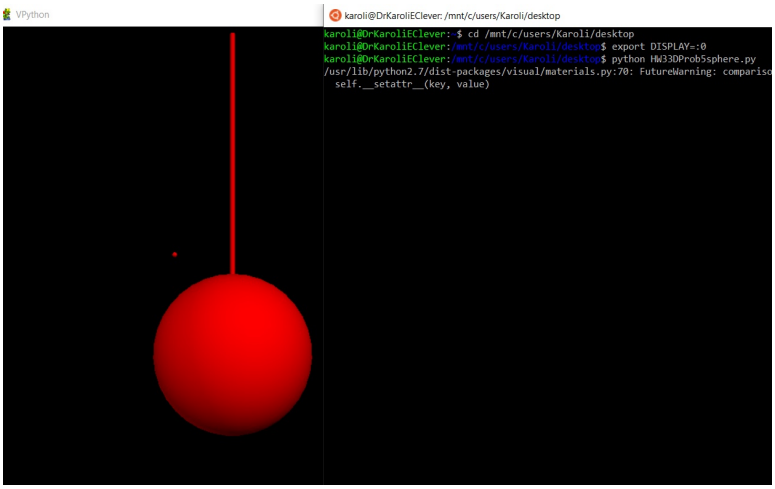

Figure 6: Digital animation of sphere and random walking particle (image: Karoli Clever, 2021).

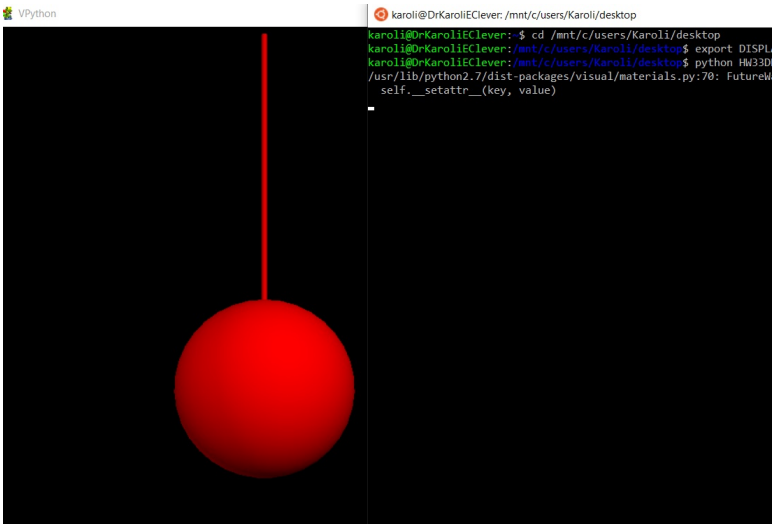

Figure 7: Digital animation of sphere where the random walking particle is either infront of or behind the sphere. In this simulation it took approximately 125 seconds for this specific particle to disappear. After further 60 seconds, the sphere didn't turn white so it must have just been at a position that wasn't visible. Team partner Rey Cervantes observed his graphics for 10 minutes with similar results, particle disappeared and was not visible for several minutes. Neither spheres turned white, according to the code when the particle would actually have been absorbed. (image: Karoli Clever, 2021).

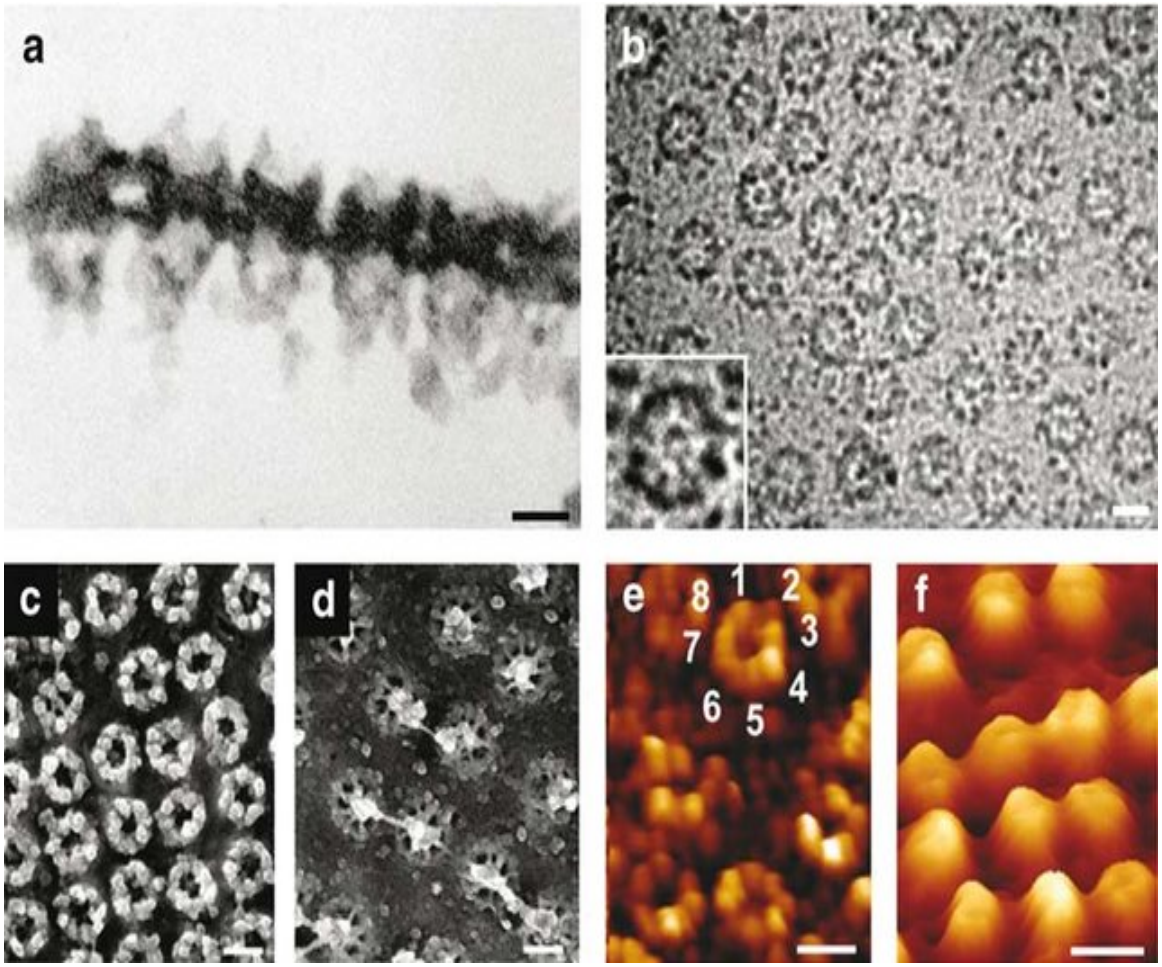

Figure 8: Imaging the nuclear pore complex shown by various microscopy techniques (Lim et al., 2006).

3 Experimental Techniques

FRAP Technique

FRAP stands for fluorescence recovery after photobleaching and is a technique used to measure the rate of 2d lateral diffusion of fluorescent labeled particles. The steps in this process can be visualized in Figure 2. First, a desired region of a surface containing mobile fluorescent molecules is exposed to a brief intense pulse of light which causes irreversible photochemical bleaching, removing the fluorescence from this area (Axelrod et al., 1976). Due to diffusion processes within this area, fluorescent molecules that were initially outside the bleached region freely make their way into the region over time. This makes for an eventual recovery in fluorescence in the bleached area, hence the name fluorescence recovery after photobleaching. By bleaching a component or organelle within a cell, we can observe the diffusion rate of molecules in and out of that component as the fluorescence recovers. Transport coefficients such as diffusion coefficients are determined by measuring the recovery rate of fluorescence (Axelrod et al., 1976).

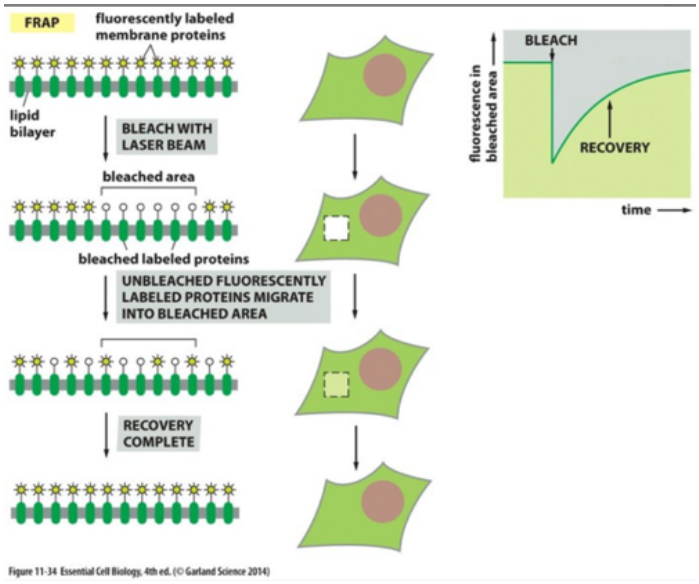

Figure 9: Depiction of FRAP procedure on a cell membrane bilayer. The molecular side view to the left corresponds with a top view to the right. Time moves on as the images go from top to bottom. A group of fluorescently labeled membrane proteins are initially bleached with a focused laser beam. Then unbleached fluorescently labeled proteins migrate into the bleached area over time. This diffusion of fluorescent molecules results in fluorescence recovery over time. If enough proteins are bleached, the overall fully recovered fluorescence intensity will be lower than before because there are still less fluorescently labeled proteins throughout the membrane. The speed of fluorescence recovery of the bleached area is directly proportional to the diffusion speed of the proteins.

Using FRAP to determine a diffusion coefficient

The goal of the assignment here is to determine the diffusion coefficient of a protein bound to the membrane but free to make 2d motion around it. The radius of the region photo-bleached for our simulated data is 8, and the radius for experimental data is 2. The fluorescent intensity at the center of the photo-bleached circle is measured as a function of time. The experimental data is in measurements.txt and the simulated data is in graphcomparison.txt. To solve for the diffusion coefficient of the experimental protein bound to the membrane, D_e, we make use of the fact that 2d diffusion is modeled by a 2d random walk. Scaling time axes of either of the data sets such that the two intensity curves are superimposed will allow us to determine the diffusion coefficient of the experimental data, D_e, utilizing the fact that we know the diffusion coefficient from the simulated data, $D_s = 0.33$.. We make use of the relationship:

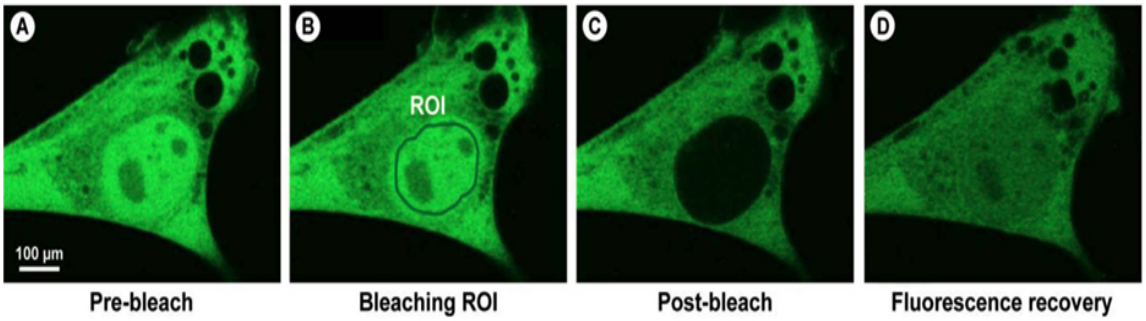

Figure 10: An example of the FRAP procedure in a myo3 cell expressing GFP-myosin 3. (A) - cell is evenly stained with fluorescence. (B) - region of interest (ROI) is selected. In this case the ROI is the nucleus of the cell. (C) - the ROI has been bleached by a high powered laser. (D) - Fluorescene in the ROI recovers through diffusion of non-bleached fluorophores. There is a decrease in the total amount of fluorescence when compared to the original fluorescent cell in image A. Ishikawa-Ankerhold et al. (2012).

$$R_e^2 \propto D_e t \tag{13}$$

which goes the same for the simulated data, and where $R_e = 2$, and $R_s = 8$.
The idea is that we can plot the intensity as a function of time and make these two data sets overlap or equal each other by scaling the time axes for one of the curves. We know that:

$$\frac{R_s^2}{R_e^2} = \frac{(4R_e)^2}{R_e} = 16 \propto \frac{D_e t_e}{D_s t_s}. \tag{14}$$

If the diffusion coefficients of the two were equal, we could make the experimental and simulated data superimpose by re-scaling the time axes. For this case that would mean multiplying t_s by 16 which is equivalent to dividing t_e by 16. This balances out the fact that the radius of simulated simulation is 4 times the experimental.
This is not the end of the problem as the diffusion coefficients D_e and D_s are not equal. Along with the difference in radius there is a difference in the timescale and this is a separate timescale factor that must be considered to make the two curves superimpose, $t_s = at_e$ where a is the scale factor. The method used to find this scale factor could have been more accurate but was done by trial and error, multiplying the timescale of the simulated data by some constant, until the two curves superimposed. I found this scale factor to be $a = 38.10$.
Now our Diffusion coefficient ratio from equation 12 looks like:

$$\frac{D_e}{D_s} \propto \frac{16t_s}{38.10t_s} = 0.42 \tag{15}$$

where the substitution $t_e = 38.10t_s$ was made.
An additional note is that D_s was calculated from the 2d FRAP simulation in the script 2ddiff.py. We make use of the diffusion random walk equation:

$$< r^2 >= 4Dt. \tag{16}$$

All the simulated particles start at a single point and diffuse from there. The mean square displacement, $< r^2 >$, is calculated as a function of time. Utilizing equation 14, $D = \frac{<r^2>}{4t}$, and so the slope of our data that makeup this ratio will be an accurate value for the diffusion coefficient of this simulation. This value was determined to be $D_s = 0.33$.
Now we can calculate D_e using equation 13:

$$D_e = (0.42)(0.33) \rightarrow \boxed{\mathrm{D}_e = 0.14} \tag{17}$$

The relationship between $D_e = 0.14$ and $D_s = 0.33$ makes sense when we plot the original fluorescent intensity curves for both without any scaling factors. As seen in figure 4, the experimental data has a lower intensity as a function of time during the early stages of intensity recovery, agreeing with the smaller diffusion coefficient value. We see in figure 5 that when the overall scaling factor 0.42 is multiplied to the timescale from the experimental data set, the experimental and simulated curves superimpose nicely. Superimposing the curves can also be done by re-scaling the simulated time axes by $1/.42 = 2.38$.

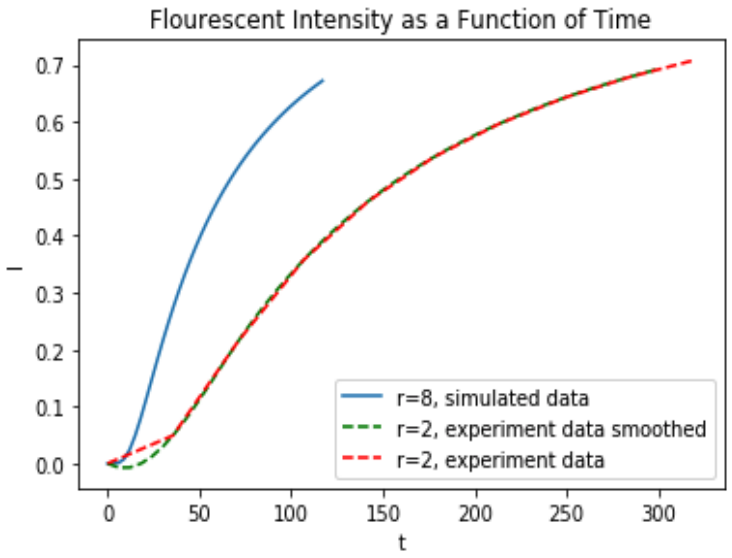

Figure 11: Plot of the original experimental and simulated FRAP intensity data. Experimental data only contains 11 data points so it was smoothed over to simulate more data points.

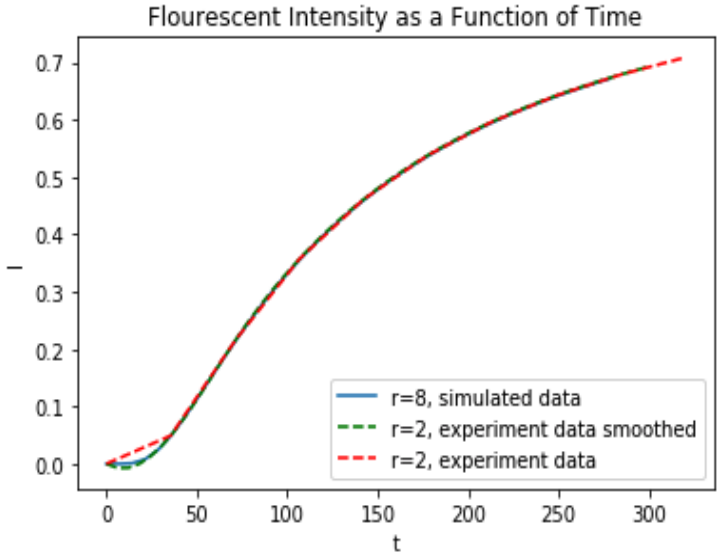

Figure 12: Plot of experimental and simulated FRAP intensity data and now the simulated data is scaled such that the intensity curve is superimposed upon the experimental data. This was done by re-scaling the time axes by 38.10/16. Similarly, to superimpose the experimental curve over the simulated curve, the experimental time axes can be re-scaled by 16/38.10.

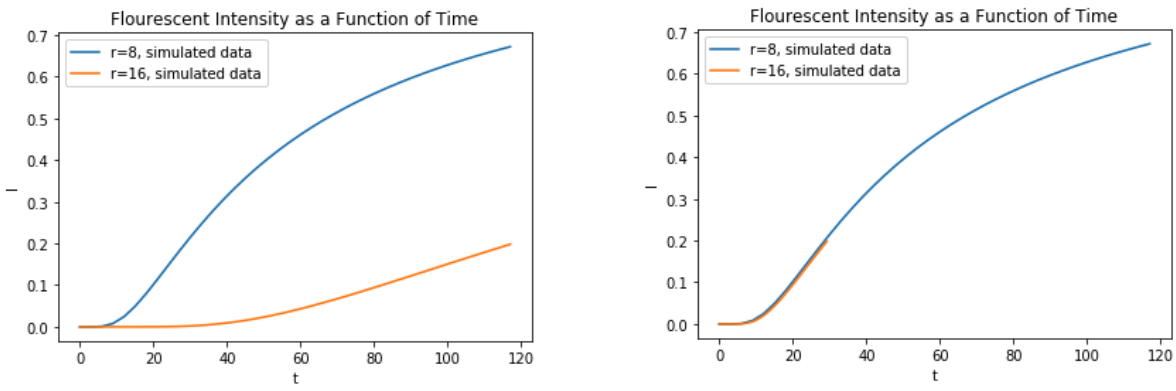

(a) (b)

Figure 13: (a) Simulated intensity data for a photobleaching radius of r = 8 and r = 16. The simulated diffusion coefficient is $D_s = 0.33$. (b) r = 16 curve is superimposed onto r = 8 curve by dividing the timescale by 4. This is possible due to the proportionality $r^2 \propto Dt$. Meaning that if the radius is 2 times as large, the timescale must be divided by $2^2 = 4$ to simulate the same intensity curve.

4 Sources and References

https://www.akadeum.com/blog/density-gradient-centrifugation

Axelrod, D., Koppel, D. E., Schlessinger, J., Elson, E., Webb, W. W. (1976). Mobility measurement by analysis of fluorescence photobleaching recovery kinetics. Biophysical journal, 16(9), 1055–1069. https://doi.org/10.1016/S0006-3495(76)85755-4

Cooney CA, Matthews HR. The isolation of satellite DNA by density gradient centrifugation. Methods Mol Biol. 1985;2:21-9. doi: 10.1385/0-89603-064-4:21. PMID: 21374168.

Cooper, Geoffrey M., and Robert E. Hausman. The cell: a molecular approach. 2004.

Farrell, R. E., Farrell, Jr. (2010). RNA Isolation Strategies. Rna methodologies : Laboratory guide for isolation and characterization. (pp. 45-80). Academic Press.

Hernandez, Victoria, "Equilibrium Density Gradient Centrifugation in Cesium Chloride Solutions Developed by Matthew Meselson and Franklin Stahl". Embryo Project Encyclopedia (2017-12-19). ISSN: 1940-5030 http://embryo.asu.edu/handle/10776/13032.

Ishikawa-Ankerhold HC, Ankerhold R, Drummen GP. Advanced fluorescence microscopy techniques–FRAP, FLIP, FLAP, FRET and FLIM. Molecules. 2012 Apr 2;17(4):4047-132. doi: 10.3390/molecules17044047. PMID: 22469598; PMCID: PMC6268795.

Lianidou, Evi, and Dave Hoon. "Circulating tumor cells and circulating tumor DNA." Principles and applications of molecular diagnostics. Elsevier, 2018. 235-281.

Lim, Roderick YH, Ueli Aebi, and Daniel Stoffler. "From the trap to the basket: getting to the bottom of the nuclear pore complex." Chromosoma 115.1 (2006): 15-26.

Murphy, Kenneth, and Casey Weaver. Janeway's immunobiology. Garland science, 2016.

https://www.nature.com/scitable/definition/nuclear-pore-279

https://www.ncbi.nlm.nih.gov/books/NBK9928

https://opentextbc.ca/anatomyandphysiologyopenstax/chapter/the-cell-membrane

https://www.PearsonEducation.com. Web. 2021

https://projects.ncsu.edu/project/bio183de/Black/membranes/membranes.html

https://www.slideshare.net/georgeoajr/density-gradient-centrifugation. Web, 2021.